

March 26, 2022

# A (Slightly Less Brutal) Method for Numerically Evaluating Structure Functions

D. Fasching

*Physics Department, University of Wisconsin-Madison, 1150 University Avenue,  
Madison, Wisconsin 53706, USA<sup>†</sup>*

## Abstract

A fast numerical algorithm for the evolution of parton distributions in  $x$  space is described. The method is close in spirit to ‘brute’ force techniques. The necessary integrals are performed by summing the approximate contributions from small steps of the integration region. Because it is a numerical evaluation it shares the advantage with brute force numerical integration that there are no restrictions placed on the functional form of the distributions to be evolved. However, an improvement in the approximation technique results in a significant reduction in the number of integration steps and a savings in time on the order of three hundred fifty. The method has been implemented for the structure functions  $F_2$  and  $g_1$  at next-to-leading order.

---

<sup>†</sup>Currently located at Lawrence Berkeley National Laboratory, MS 50-348, 1 Cyclotron Road, Berkeley CA 94720, USA.

# 1 Introduction

Much of the information which can be gained from studying collisions at high energy hadron colliders can only be extracted from the data if one has previous knowledge of hadronic structure. Presently this knowledge is not available by direct calculation and so must be obtained by other means. Dedicated high energy lepton-proton deep inelastic scattering, DIS, experiments provide the means to measure this structure. The structure functions which are measured in such experiments are essentially the cross-sections and hence are not directly applicable to other processes. However, they can be related to parton distributions which are universal and which can therefore be used to predict, for example, production rates in the more complicated environment of a hadron collider. There are other reasons why determining parton distributions is of interest. For example, one hopes that at some point they will be accessible by direct calculation. Such predictions will then need to be compared with experimental measurements. In addition, the proper evaluation of DIS sum rules relies on the same formalism by which the parton distributions are extracted. These reasons, along with the large and growing body of DIS data, make a strong case for efficient tools for determining parton distributions.

Structure functions are related to parton distributions via the operator product expansion. Within this framework, the structure function at some scale,  $Q^2$ , is expressed in terms of a convolution of parton distributions with coefficient functions which can be calculated perturbatively [1]. For the case of charged lepton scattering in the one photon exchange approximation we have,

$$F_i(x, Q^2) = a_i(x) \left\{ \langle e^2 \rangle \left[ \Sigma(Q^2) \otimes_x C_i^\Sigma + G(Q^2) \otimes_x C_i^G \right] + q^{NS}(Q^2) \otimes_x C_i^{(NS)} \right\}, \quad (1)$$

where  $f \otimes_x q \equiv \int_x^1 \frac{dz}{z} f\left(\frac{x}{z}\right) q(z)$ ,  $a_2 = a_L = x$ ,  $a_1 = \frac{1}{2}$ ,  $\Sigma(x, Q^2)$ ,  $G(x, Q^2)$  and  $q^{NS}(x, Q^2)$  are the quark singlet, gluon and nonsinglet distributions, respectively, the  $C_i$  are the coefficient functions and  $\langle e^2 \rangle$  is the mean squared charge of the involved quarks. In (1) the factorization scale and the scale at which the structure function is defined have been implicitly set equal to each other. Because this will always be the case in this paper, the more general expression is not given. For  $g_1$ ,  $a_1 = \frac{1}{2}$  and the parton distributions are substituted by their polarized counterparts,  $\Delta\Sigma$ ,  $\Delta G$  and  $\Delta q^{NS}$ . Eq. (1) can be taken as a definition of the parton distributions. The distributions, therefore, depend on the details of the calculation of the coefficient functions, which are not unique.

Though the parton distributions can not presently be calculated, their dependence on  $Q^2$  is predictable for high enough values of  $Q^2$ . Because of this, the large body of DIS data currently available, extending up to  $5 \times 10^4 \text{ GeV}^2$  and down to  $x = 10^{-5}$ , can be used together in a single global fit of the distributions. Their  $Q^2$  dependence is given by the DGLAP equations [2]. Because the QCD processes which govern this dependence do not act on flavor indices, the (flavor) singlet distribution, in which these indices have been summed out, and the nonsinglet distribution behave differently. In

particular, the gluon distribution, which also does not carry flavor, can have no effect on the nonsinglet distribution in the perturbative evolution. Thus, in the nonsinglet sector we have

$$\frac{d}{dt}q^{NS}(x,t) = \frac{\alpha_s(t)}{4\pi}P_{qq}^{NS}(\alpha_s(t)) \otimes_x q^{NS}(t), \quad (2)$$

where  $t = \ln \frac{Q^2}{\Lambda^2}$  and  $P^{NS}(x, \alpha_s(Q^2))$  is the nonsinglet quark splitting function, which can be calculated in perturbative QCD. The coupled evolution equations in the singlet sector are

$$\begin{aligned} \frac{d}{dt}\Sigma(x,t) &= \frac{\alpha_s(t)}{4\pi} \left[ P_{qq}^{\Sigma}(\alpha_s(t)) \otimes_x \Sigma(t) + P_{qg}(\alpha_s(t)) \otimes_x G(t) \right], \\ \frac{d}{dt}G(x,t) &= \frac{\alpha_s(t)}{4\pi} \left[ P_{gq}(\alpha_s(t)) \otimes_x \Sigma(t) + P_{gg}(\alpha_s(t)) \otimes_x G(t) \right]. \end{aligned} \quad (3)$$

The present state of knowledge of the splitting functions and coefficient functions allows for a next-to-leading order, NLO, treatment of both the polarized and unpolarized structure functions. For a concise review of the state of the art of these calculations see reference [3].

The relationship (1-3) between the objects which are parameterized, the parton distributions at a fixed scale, and the data to which they are fit, structure function data over a wide kinematic range, is quite complicated. In fact, these equations do not have analytic solutions. Because of this several techniques, including integral transforms, polynomial expansions and numerical methods, have been employed to obtain approximate solutions.

The most popular of the polynomial expansion techniques involves expanding the splitting and coefficient functions, as well as the parton distributions, in Laguerre polynomials [4, 5]. In this technique, the convolutions (1-3) reduce to a sum of products of Laguerre polynomials. A study of the Laguerre method [6] showed that one could obtain accurate results quickly in the range  $0.01 < x < 0.8$ . Outside of this range, it was observed that the Laguerre expansion no longer describes the functions and so the method breaks down. Given that polarized scattering data is available down to  $x = 3 \times 10^{-3}$  [7] and unpolarized data is available down to  $x = 10^{-5}$  [8, 9], this method is no longer practical.

Another standard procedure is to transform the entire set of equations into moment space via a Mellin transformation. The convolutions of the  $x$  dependent functions appear as products of their moment space counterparts. This simpler set of equations has a closed form solution which can be transformed back to  $x$  space for comparison with data. This technique is typically much faster than a direct numerical evaluation in  $x$  space, which is another popular technique.

A ‘brute force’ numerical integration method was discussed in references [10, 11]. In this method the convolutions in Eqs. (1-3) are performed by straightforward numerical integration, dividing the integration region into small steps and summing

their approximate contributions to the integral,

$$P \otimes_x q = \sum_j \int_{x_j}^{x_{j+1}} \frac{dz}{z} P(z) q\left(\frac{x}{z}\right)_j, \quad (4)$$

$$\approx \sum_j \frac{\delta x_j}{x_{j+1/2}} P(x_{j+1/2}) q\left(\frac{x}{x_{j+1/2}}\right). \quad (5)$$

Here,  $P$  represents a general splitting or coefficient function,  $q$  is a general parton distribution,  $\delta x_j = x_{j+1} - x_j$  and  $x_{j+1/2}$  lies somewhere between  $x_j$  and  $x_{j+1}$ . Similarly, the differential in  $t$  is approximated by a finite difference. Eq. (2) becomes

$$\Delta q^{\text{NS}}(x, t_{l\pm 1}) \approx \Delta q^{\text{NS}}(x, t_l) + \delta t_l \cdot \frac{\alpha_s(t_l)}{4\pi} \cdot \sum_j \frac{\delta x_j}{x_{j+1/2}} P(x_{j+1/2}, \alpha_s(t_l)) \cdot q\left(\frac{x}{x_{j+1/2}}, t_l\right), \quad (6)$$

where  $\delta t_l = t_{l\pm 1} - t_l$ . Similar expressions hold in the singlet sector. No restrictions are imposed on the functional form of the distributions because all of the functions are evaluated numerically. For the same reason, as was pointed out and in fact implemented in reference [11], it is well suited for solving the nonlinear modified evolution equations [12] which take recombination effects into account.

Because the integral on the left hand side of Eq. (4) must be performed with each  $x$  step value as the lower limit, the number of times the integral on the right hand side must be performed is roughly proportional to the square of the number of  $x$  steps. This must be repeated for each point in the  $t$  grid. For the implementation of reference [11] an accuracy of 2% on unpolarized distributions in the kinematic range relevant to the HERA collider experiments requires 1000 steps in  $\ln(x)$ , with a running time of roughly one hour.<sup>1</sup> This is acceptable to evolve a fixed set of distributions but not practical for performing fits of parton distributions where the evolution may need to be repeated several hundred times. In addition, the freedom to try different functional forms, to try different data sets, or to perform other checks on the fit result is not easily accommodated by such a time consuming procedure. Below, a slightly less ‘brutal’ numerical technique is described which has the advantages of the brute force method but for which the running time is considerably reduced, making it more useful for performing fits.

## 2 Semianalytic Solution

Up to NLO, the splitting and coefficient functions found in the references of [3] can be cast in the form

$$P(x) = P_a(x) + \sum_{k=0}^1 P_k f_{k+}(x) + P_\delta \delta(1-x), \quad (7)$$

---

<sup>1</sup>The program was run on an AlphaServer 2100 4/200.

where  $P_0$ ,  $P_1$  and  $P_\delta$  are numerical coefficients and  $P_a(x)$  is a function of  $x$ . The ‘plus’ distributions,

$$f_{k+}(x) = \left( \frac{\ln^k(1-x)}{1-x} \right)_+, \quad (8)$$

are defined via the following integral over the interval 0 to 1,

$$\int_0^1 \left( \frac{\ln^k(1-z)}{1-z} \right)_+ g(z) dz = \int_0^1 \frac{\ln^k(1-z)}{1-z} [g(z) - g(1)] dz. \quad (9)$$

Though the method to be described does not depend on the precise form of the splitting and coefficient functions, it is instructive to separate the convolution integrals into the pieces suggested by (7).

## 2.1 Basic Method and Convolutions with $P_a(x)$

As in the brute force method, the starting point is Eq. (4). We would like to approximate the integrand on the right hand side of that equation as well as possible. In the brute force method the value of the integrand throughout the bin is approximated by its value at the bin center. In what will be called the semianalytic method it is first noted that approximating the integrals of the splitting and coefficient functions is not necessary because their functional dependencies are known. They could, for example, be explicitly integrated throughout the bin and the result multiplied by the value of the parton distribution at the bin center. There is a technical difficulty associated with this which will be described in the next section. For now we simply state that one solution to this difficulty is to instead approximate the distribution with a linear interpolation in  $\frac{1}{z}$  between its values at each pair of adjacent points in the  $x$  grid,  $z = x_j$  and  $z = x_{j+1}$ ,

$$q\left(\frac{x}{z}\right)_j \approx \frac{q\left(\frac{x}{x_{j+1}}\right) - q\left(\frac{x}{x_j}\right)}{\left(\frac{x}{x_{j+1}} - \frac{x}{x_j}\right)} \cdot \left(\frac{x}{z} - \frac{x}{x_j}\right) + q\left(\frac{x}{x_j}\right). \quad (10)$$

Substituting this expression into the right hand side of Eq. (4) and taking only the  $P_a$  piece of Eq. (7), we arrive at the expression for the convolution of  $P_a(z)$  with  $q\left(\frac{x}{z}\right)$  in the semianalytic method,

$$P_a \otimes_x q \approx \sum_j \left\{ W_1 \int_{x_j}^{x_{j+1}} dz \frac{P_a(z)}{z} + W_2 \int_{x_j}^{x_{j+1}} dz \frac{P_a(z)}{z^2} \right\}, \quad (11)$$

where

$$W_1 = \frac{x_{j+1} q\left(\frac{x}{x_{j+1}}\right) - x_j q\left(\frac{x}{x_j}\right)}{x_{j+1} - x_j}, \quad (12)$$

$$W_2 = -\frac{x_j x_{j+1}}{x_{j+1} - x_j} \left[ q\left(\frac{x}{x_{j+1}}\right) - q\left(\frac{x}{x_j}\right) \right]. \quad (13)$$

The integrals appearing in (11) need only be evaluated once for each  $x$  step. The  $W_k$  must be evaluated for each pairwise combination of  $x$  steps at each  $t$  step of the evolution. If a fit is being performed, the  $W_k$  must be reevaluated each time a parameter is changed which affects the value of  $q$ .

This method, in addition to retaining all of the information of the splitting and coefficient functions, improves the approximation of the parton distributions (which can only be known approximately in any case) compared to that used in the brute force method. The resolution of the  $x$  grid needed to obtain a reasonable approximation is determined by the quality of the data. Beyond a certain resolution, the accuracy of the approximation will exceed what the data can tell us about the distributions. In the implementation of this method described in [13] which treated only  $g_1$ , the indefinite integrals  $\int dz \frac{P_a(z)}{z}$  and  $\int dz \frac{P_a(z)}{z^2}$  were explicitly worked out and were also evaluated numerically by gaussian quadrature. Differences between the results were negligible, and so in this implementation, which includes  $F_2$  as well, all integrals are performed numerically. The dilogarithm,  $\text{Li}_2(x)$ , which occurs in the splitting and coefficient function has been evaluated using its power series form. Because performing numerical integrals involving this power series can be time consuming for  $|x| \sim 1$  the substitutions

$$\begin{aligned}\text{Li}_2(x) &= \frac{\pi^2}{6} - \ln(x)\ln(1-x) - \text{Li}_2(1-x), \\ \text{Li}_2(x) &= -\text{Li}_2\left(\frac{-x}{1-x}\right) - \frac{1}{2}\ln^2\left(\frac{1}{1-x}\right),\end{aligned}$$

have been used for  $x \sim 1$  and  $x \sim -1$ , respectively.

## 2.2 Convolutions with the Plus Terms

Apart from a minor technical detail, the plus terms are treated in the same way. Starting with the definition in Eq. (9), we can write

$$f_{k+} \otimes_x q = \int_x^1 dz \frac{\ln^k(1-z)}{1-z} \left[ \frac{q\left(\frac{x}{z}\right)}{z} - q(x) \right] - q(x) \int_0^x dz \frac{\ln^k(1-z)}{1-z}. \quad (14)$$

Again using Eqs. (4) and (10) we have

$$\begin{aligned}P_k f_{k+} \otimes_x q &= P_k \left\{ \sum_j \left[ W_1 \int_{x_j}^{x_{j+1}} dz \frac{\ln^k(1-z)}{z(1-z)} + W_2 \int_{x_j}^{x_{j+1}} dz \frac{\ln^k(1-z)}{z^2(1-z)} \right] \right. \\ &\quad \left. - q(x) \int_0^1 dz \frac{\ln^k(1-z)}{1-z} \right\}.\end{aligned} \quad (15)$$

Because each of the integrals appearing in (15) diverges if the integration region includes  $z = 1$ , the contribution from the last step of integration must be evaluated

with care. For the case of a grid of  $N$  steps in  $x$ , the procedure is to first perform the sum on the right hand side of (15) up to  $j = N - 1$  and to perform the integral of the last term up to  $z = x_N$  only. To obtain the contribution from the  $N^{th}$   $x$  step,  $x_N < z < 1$ , the three terms on the right hand side of (15) are first combined. The  $\frac{1}{1-z}$  does not appear in the resulting expression, and so the integral can be explicitly performed. For  $k = 0$  and  $k = 1$  the contributions from the  $N^{th}$   $x$  step are

$$P_0 [f_{0+} \otimes_x q]_N = P_0 \left\{ -q(x) [1 + \ln(x_N)] + q\left(\frac{x}{x_N}\right) \right\} \quad (16)$$

and

$$\begin{aligned} P_1 [f_{1+} \otimes_x q]_N = & P_1 \left\{ \frac{x_N}{1 - x_N} \left[ -q(x) + q\left(\frac{x}{x_N}\right) \right] \left[ \frac{1 - x_N}{x_N} \ln(1 - x_N) + \ln(x_N) \right] \right. \\ & \left. + q(x) [-\text{Li}_2(1) + \text{Li}_2(x_N)] \right\}. \end{aligned} \quad (17)$$

Because all of the parton distributions vanish at  $x = 1$ , their approximation with a linear interpolation, in addition to improving the accuracy, is responsible for the cancellation of the  $\frac{1}{1-z}$  divergence. Assembling the pieces from Eqs. (11), (15) and (17), and including the contribution from the delta function term in Eq. (7), gives the semianalytic expression for the convolution integrals.<sup>2</sup>

In [13], a detailed comparison of the performance of the brute force and semianalytic methods was performed for  $g_1$  in the range  $0.0045 < x < 1.0$  and  $1 \text{ GeV}^2 < Q^2 < 60 \text{ GeV}^2$ . As the number of  $x$  steps was increased, both methods converged on the same result. To obtain the same accuracy within a few tenths of a percent, which is sufficient for the  $g_1$  data,  $30 \ln(Q^2)$  steps and  $40 (1280) \ln(x)$  steps were required for the semianalytic (brute force) methods. The semianalytic evolution was about 350 times more efficient than the brute force method, requiring approximately 4 seconds to complete.<sup>3</sup> The following section on performance will focus on the convergence of the semianalytic method and on the behavior of the structure functions and evolved parton distributions.

### 3 Performance

For the case of  $F_2$  the MRS(A) set of distributions [14], defined in the  $\overline{MS}$  renormalization scheme, was used as input to the evolution. The starting scale was  $4.0 \text{ GeV}^2$  and the distributions were evaluated down to  $x = 10^{-4}$  in the range  $4.0 \text{ GeV}^2 < Q^2 < 10^4 \text{ GeV}^2$ . The evolution was performed in 200 logarithmically distributed  $Q^2$  steps. Several different numbers of  $x$  steps, also distributed logarithmically, were tried. A

---

<sup>2</sup>Due to a typographical error in the presentation of this result in reference [13], the full expression is repeated in appendix A.

<sup>3</sup>Both methods were run on a SUN SPARC 10 workstation when making this comparison.

reference set of distributions was first calculated using 496  $x$  steps. Distributions calculated with 248, 124, and 62  $x$  steps were then compared with these. The results are shown in Figs. 1-4 for  $F_2(x)$ ,  $u_v(x)$ ,  $S(x)$  and  $G(x)$  where  $u_v(x)$  is the valence up quark distribution and  $S(x)$  is the *total* sea quark distribution.

In these figures, the difference between the reference set and the other sets has been normalized to the reference set and plotted as a function of  $x$  at various  $Q^2$  values. Note that all the quantities converge rapidly in the region from  $x = 10^{-4}$  up to some high value, which depends on the quantity in question. Beyond this value, there is a strong dependence of the result on the number of  $x$  steps. Because the spacing in  $x$  is logarithmic, this is not surprising. The situation could presumably be improved by increasing the density of points in the high  $x$  region. For example, there are 9 points with  $x > 0.5$  for the case of 124 steps. Comparing the 124 step and 248 step results for  $F_2$ , we see that doubling this number to 18 would produce the same accuracy at  $x = 0.7$  as was previously obtained at  $x = 0.5$ . This is a modest increase in the total number of steps and increases the running time from just under to just over two minutes. In [6] a linear step size was used at high  $x$ .

Similar statements can be made for the parton distributions, though for the gluon and sea quark distributions convergence on an accurate result is not as rapid as for  $F_2$  and  $u_v$ . However, if one is performing a fit of parton distributions, it is only the accuracy with which  $F_2$  is extracted which will influence the fit parameters. The convergence of the parton distributions is not directly relevant to selecting a step size in  $x$  and therefore does not influence the time required to perform the fit. If one only wants to evolve a fixed set of distributions to a high accuracy, without the iterations necessary to perform a fit, a large number of  $x$  steps can be used while still keeping a reasonable running time. In Fig. 5 a similar accuracy study is presented for  $g_1$ .

Figs. 6 and 7 show both the polarized and unpolarized parton distributions at two values of  $Q^2$ . For the polarized distributions, set A from [15] were used as input. As in the unpolarized case, the starting distributions were defined at 4 GeV<sup>2</sup> in the  $\overline{MS}$  scheme. The polarized distributions were evaluated down to  $x = 10^{-3}$  in the range 4 GeV<sup>2</sup> <  $Q^2$  < 100 GeV<sup>2</sup> with 62  $\ln(x)$  steps and 50  $\ln(Q^2)$  steps. The unpolarized distributions which are displayed in Fig. 6 were evaluated with 496  $\ln(x)$  steps and 200  $\ln(Q^2)$  steps. The structure functions subsequently derived from these parton distributions are shown in Figs. 8-11. In Figs. 8 and 9 one can directly see the logarithmic  $Q^2$  behavior of the structure functions at various values of  $x$ . A comparison shows that the sizes of the slopes normalized to the structure function value are similar for the two structure functions. At the lowest values of  $x$  the behavior of the two structure functions is quite different; both have slopes which are similar in magnitude but opposite in sign. This is consistent with expectations, the density of partons in the low  $x$  region being dominated by the sea quark and gluon distributions. As the resolution of the probe increases, more partons are seen, but their helicity is not always remembered by the processes which generate them. Because the  $Q^2$  behavior of  $F_2$  and  $F_1$  are similar, these plots are also a dramatic



illustration of the danger in the low  $x$  region of assuming  $\frac{g_1}{F_1}$  is independent of  $Q^2$ , as has been done in evaluating the first moment of  $g_1(x, Q^2)$ ,  $\Gamma_1(Q^2)$  [7, 16]. The differing low  $x$  behavior of these structure functions is evident from another point of view in the plots of  $xF_2(x)$  and  $xg_1(x)$  in Figs. 10 and 11. Here we can also see that the  $Q^2$  slope of  $F_2$  turns over around  $x = 0.12$ , which is just above the highest  $x$  value plotted in Fig. 8. The  $Q^2$  slope of  $g_1$  turns over twice, behaving as  $F_2$  in the valence region but becoming negative where the sea dominates. Finally, in Fig. 10  $F_2(x, 25\text{GeV}^2)$  (scaled by a factor of 50) is also plotted in order to facilitate a comparison with the same quantity plotted in reference [17].

## 4 Conclusions

A rapid method for the evolution of parton distributions in  $x$  space has been presented. As a numerical technique, it places no restrictions on the form of the distributions to be evolved. This freedom, as well as its ability to accommodate the evolution equations modified for recombination effects, may prove useful as the kinematic range of the data grows and its statistical accuracy improves. Pending a careful numerical analysis of the results, one can see now that the evolved distributions and the structure functions presented here compare favorably with similar figures presented in references [15] and [17].<sup>4</sup>

### Acknowledgments

Many thanks to Mayda Velasco and Stephen Trentalange for proofreading this text and for many useful comments. Kind thanks also to W.J. Stirling and T. Gehrmann for providing the FORTRAN code for the parton distributions used here.

## A Form of the Convolution Integral in the Semi-analytic Method

Eq. (20) gives the full expression of the semianalytic convolution of a splitting function or coefficient function of the form

$$P(x) = P_a(x) + \sum_{k=0}^1 P_k \cdot \left( \frac{\ln^k(1-x)}{1-x} \right)_+ + P_\delta \delta(1-x), \quad (18)$$

with a parton distribution approximated on an  $x$  grid by

$$q\left(\frac{x_i}{z}\right)_j = \frac{q\left(\frac{x_i}{x_{j+1}}\right) - q\left(\frac{x_i}{x_j}\right)}{\left(\frac{x_i}{x_{j+1}} - \frac{x_i}{x_j}\right)} \cdot \left(\frac{x_i}{z} - \frac{x_i}{x_j}\right) + q\left(\frac{x_i}{x_j}\right), \quad (19)$$

---

<sup>4</sup>The code may be obtained from the author via email at fasching@wisconsin.cern.ch.

where  $j$  is the  $x$  grid index,  $x_j$  and  $x_{j+1}$  are the upper and lower boundaries of step  $j$  and  $x_i$  is the lower limit of the integration region. If the integration region has been divided into  $N$  steps in  $x$ , with  $x_{N+1} = 1$ , we have

$$\begin{aligned}
P \otimes_{x_i} q &= P_\delta q(x_i) \\
&+ \sum_{j=i}^N \int_{x_j}^{x_{j+1}} \left[ W_1 \frac{P_a(z)}{z} + W_2 \frac{P_a(z)}{z^2} \right] dz \\
&+ \sum_{k=0}^1 P_k \sum_{j=i}^{N-1} \int_{x_j}^{x_{j+1}} \left[ W_1 \frac{\ln^k(1-z)}{z(1-z)} + W_2 \frac{\ln^k(1-z)}{z^2(1-z)} - q(x_i) \frac{\ln^k(1-z)}{1-z} \right] dz \\
&+ P_0 \left\{ -q(x_i) [1 + \ln(x_N)] + q\left(\frac{x_i}{x_N}\right) + q(x_i) \ln(1-x_i) \right\} \\
&+ P_1 \left\{ \frac{x_N}{1-x_N} \left( -q(x_i) + q\left(\frac{x_i}{x_N}\right) \right) \left( \frac{1-x_N}{x_N} \ln(1-x_N) + \ln(x_N) \right) \right. \\
&\quad \left. + q(x_i) (-\text{Li}_2(1) + \text{Li}_2(x_N)) + \frac{1}{2} q(x_i) \ln^2(1-x_i) \right\}, \tag{20}
\end{aligned}$$

where  $W_0$  and  $W_1$  are defined in Eqs. (12) and (13). Evaluating a structure function at NLO at a single  $Q^2$  value involves evaluating (20) for each of the  $N$  values of  $x_i$  for each of the involved splitting and coefficient functions.

## References

- [1] K. G. Wilson, Phys. Rev. 179 (1969) 1499.
- [2] V. N. Gribov and L. N. Lipatov, Sov. J. Nucl. Phys. 15 (1972) 438. G. Altarelli and G. Parisi, Nucl. Phys. B126 (1977) 298. Yu. L. Dokshitzer, Sov. Phys. JETP 46 (1977) 641.
- [3] W. L. van Neerven, hep-ph/9609243.
- [4] W. Furmanski and R. Petronzio, Nucl. Phys. B195, (1982) 237.
- [5] G. P. Ramsey, J. Comp. Phys. 60 (1992).
- [6] S. Kumano and J. T. Londergan, Comp. Phys. Comm. 69 (1992) 373.
- [7] SMC, B. Adeva *et al.*, Phys. Lett. B302 (1993) 533; SMC, D. Adams *et al.*, Phys. Lett. B329 (1994) 399, *erratum* Phys. Lett. B339 (1994) 332; Phys. Lett. B357 (1995) 248.
- [8] The H1 Collaboration, hep-ex/9603004.
- [9] The Zeus Collaboration, hep-ex/9607002.

- [10] G. P. Ramsey, PhD thesis, Illinois Institute of Technology (1992).
- [11] S. Kumano and M. Miyama, Saga University preprint, (1995) SAGA-HE-81-95.
- [12] A. H. Mueller and J. Qiu, Nucl. Phys. B268 (1996) 427.
- [13] D. Fasching, PhD thesis, Northwestern University, 1996.
- [14] A. D. Martin, W. J. Stirling and R. G. Roberts, Phys. Rev. D50 (1994) 6734.
- [15] T. Gehrmann and W. J. Stirling, Phys. Rev. D53 (1996) 6100.
- [16] E143 Collaboration, Phys. Rev. Lett. 74 (1995) 346; Phys. Rev. Lett. 75 (1995) 25.
- [17] A. D. Martin, W. J. Stirling and R. G. Roberts, hep-ph/9409257.

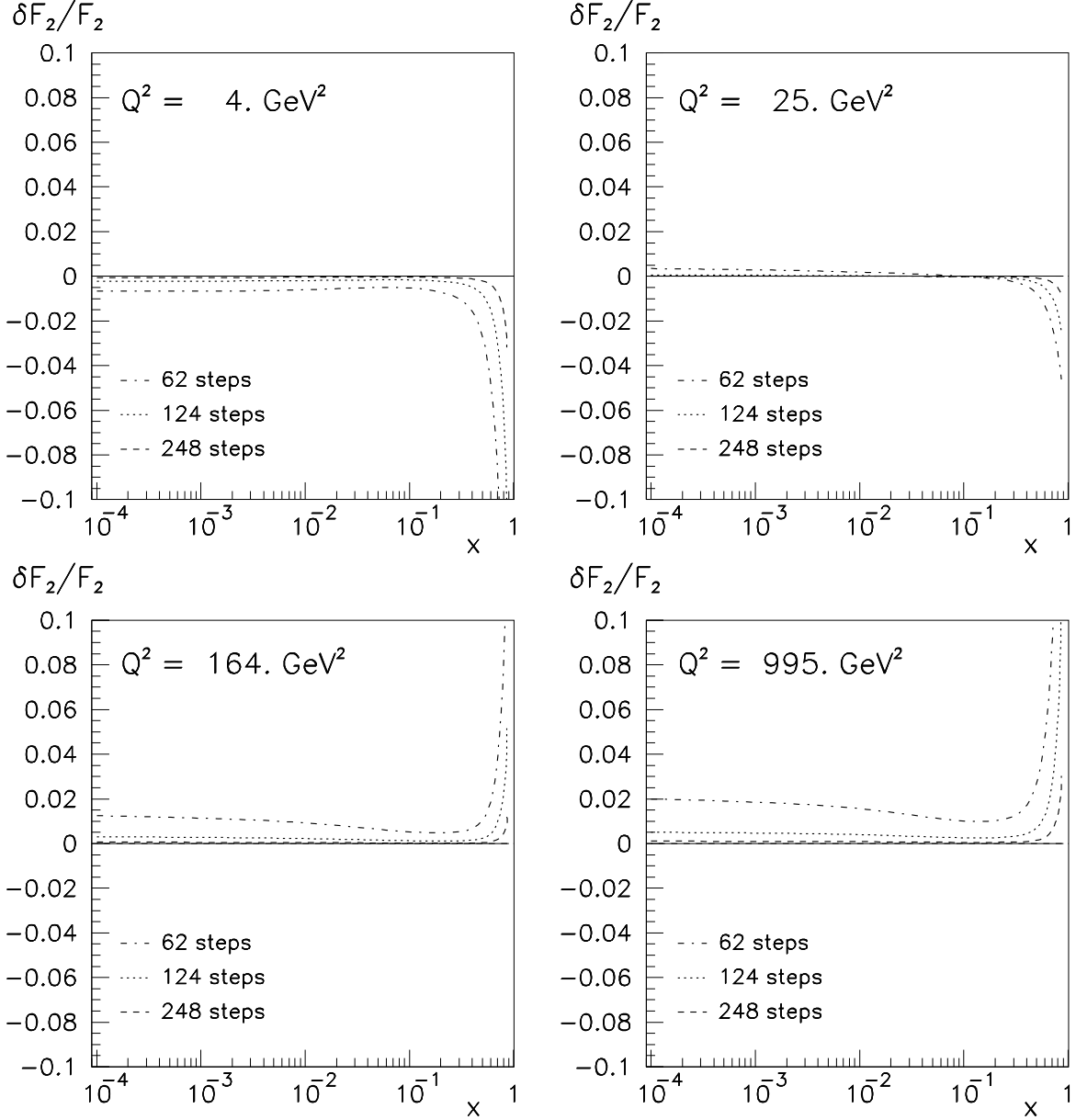


Figure 1: Results for  $F_2(x)$  from the evolution procedure described in the text at four  $Q^2$  values. The deviation of various results from a reference result, normalized to the reference result, is plotted. The reference result was calculated with  $496 \ln(x)$  steps and  $200 \ln(Q^2)$  steps. The number of  $x$  steps used to obtain the other results is indicated on the figure. The MRS(A) [14] set of parton distributions at  $4 \text{ GeV}^2$  was used as input.

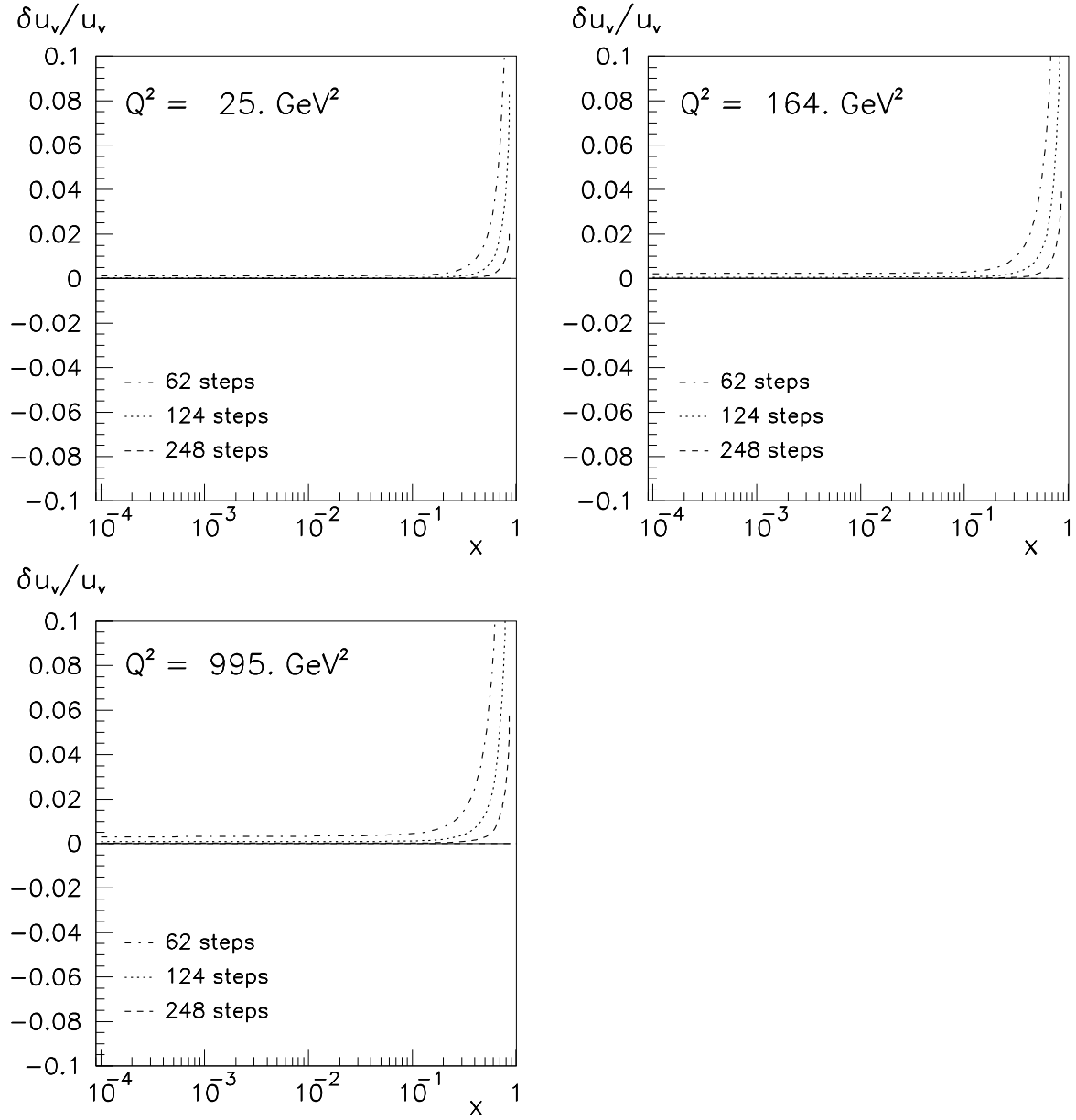


Figure 2: As in Fig. 1, but for the distribution  $u_v(x)$ .

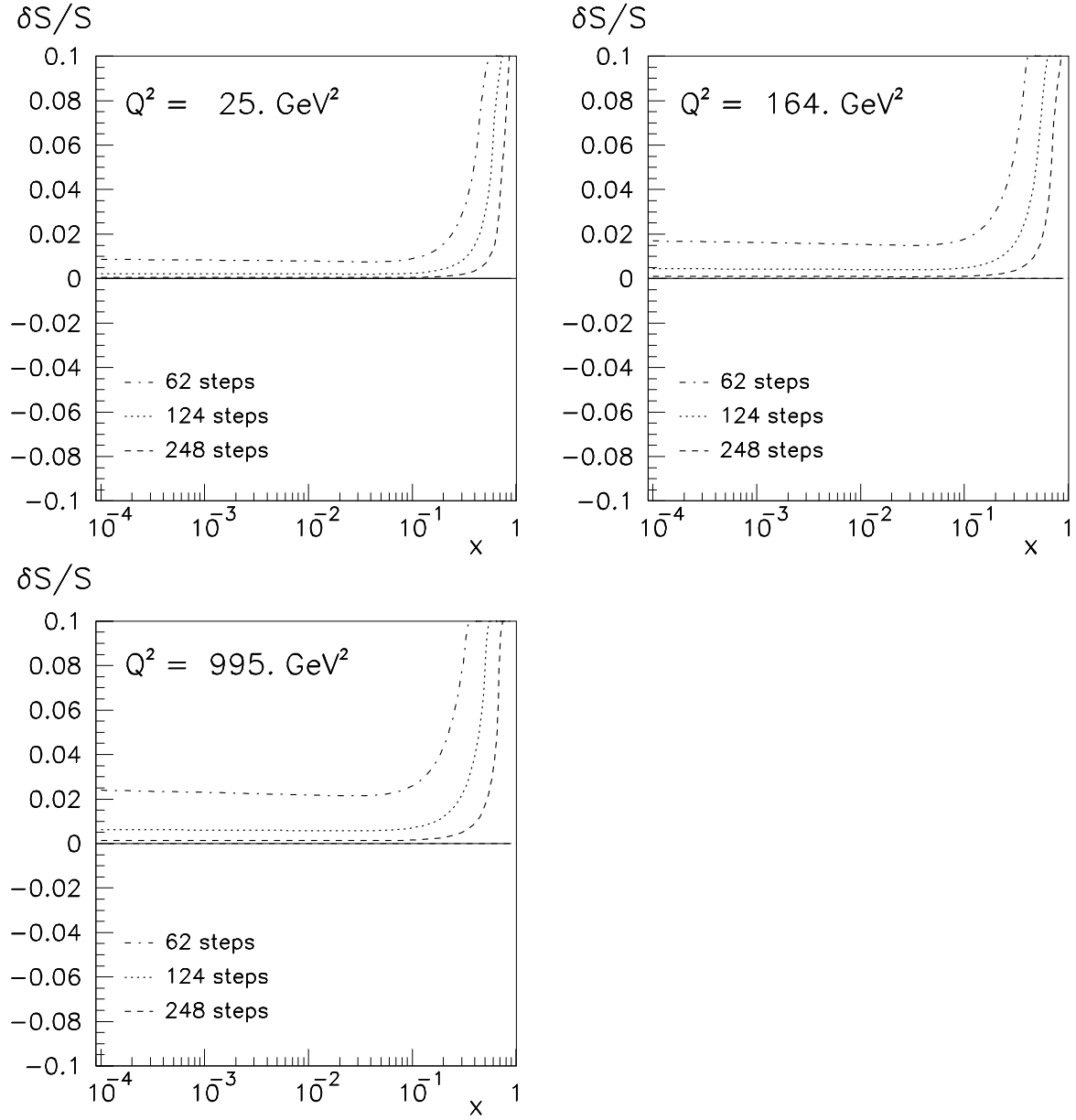


Figure 3: As in Fig. 1, but for  $S(x)$ , the total sea quark distribution.

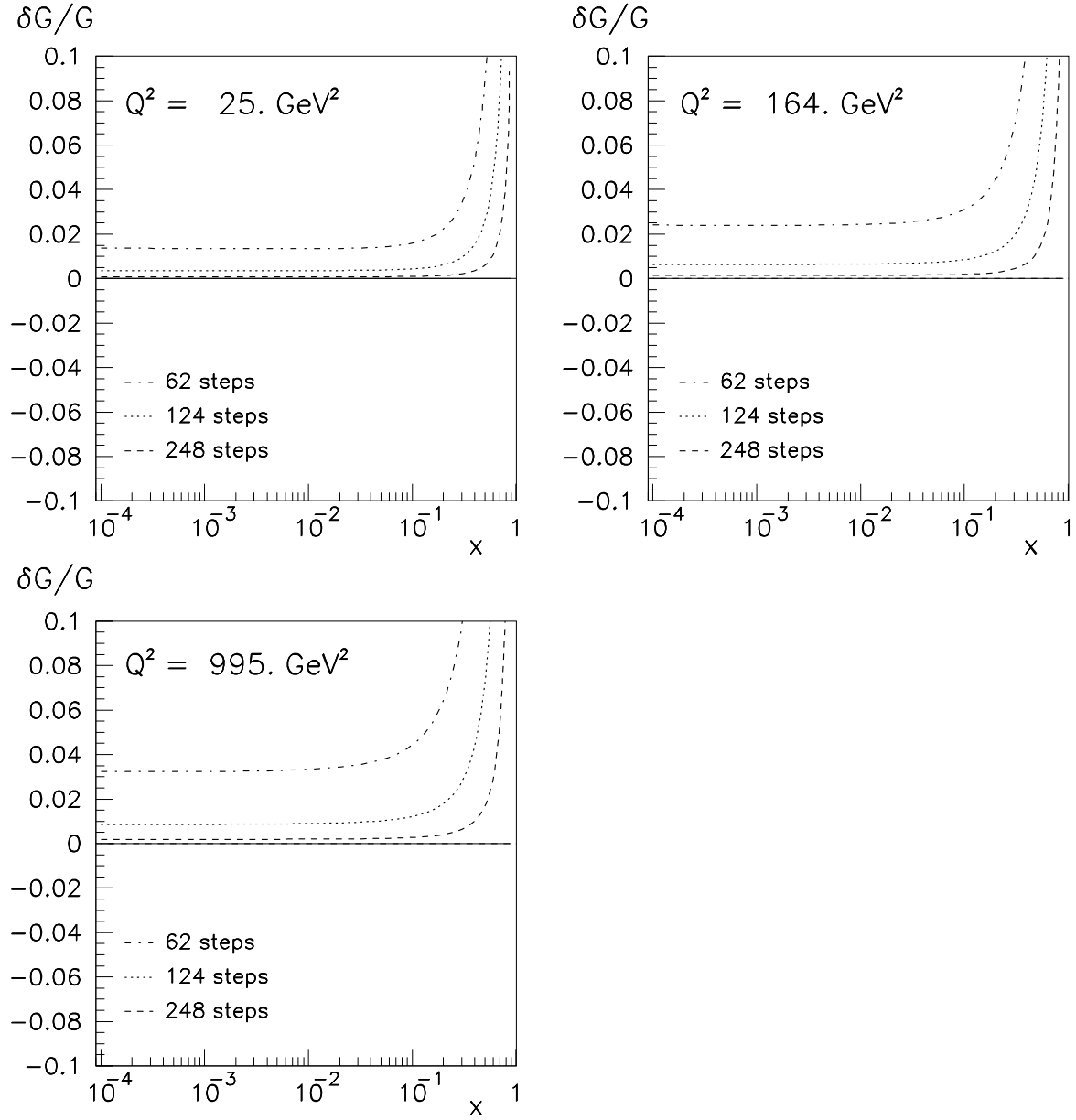


Figure 4: As in Fig. 1, but for  $G(x)$ , the gluon distribution.

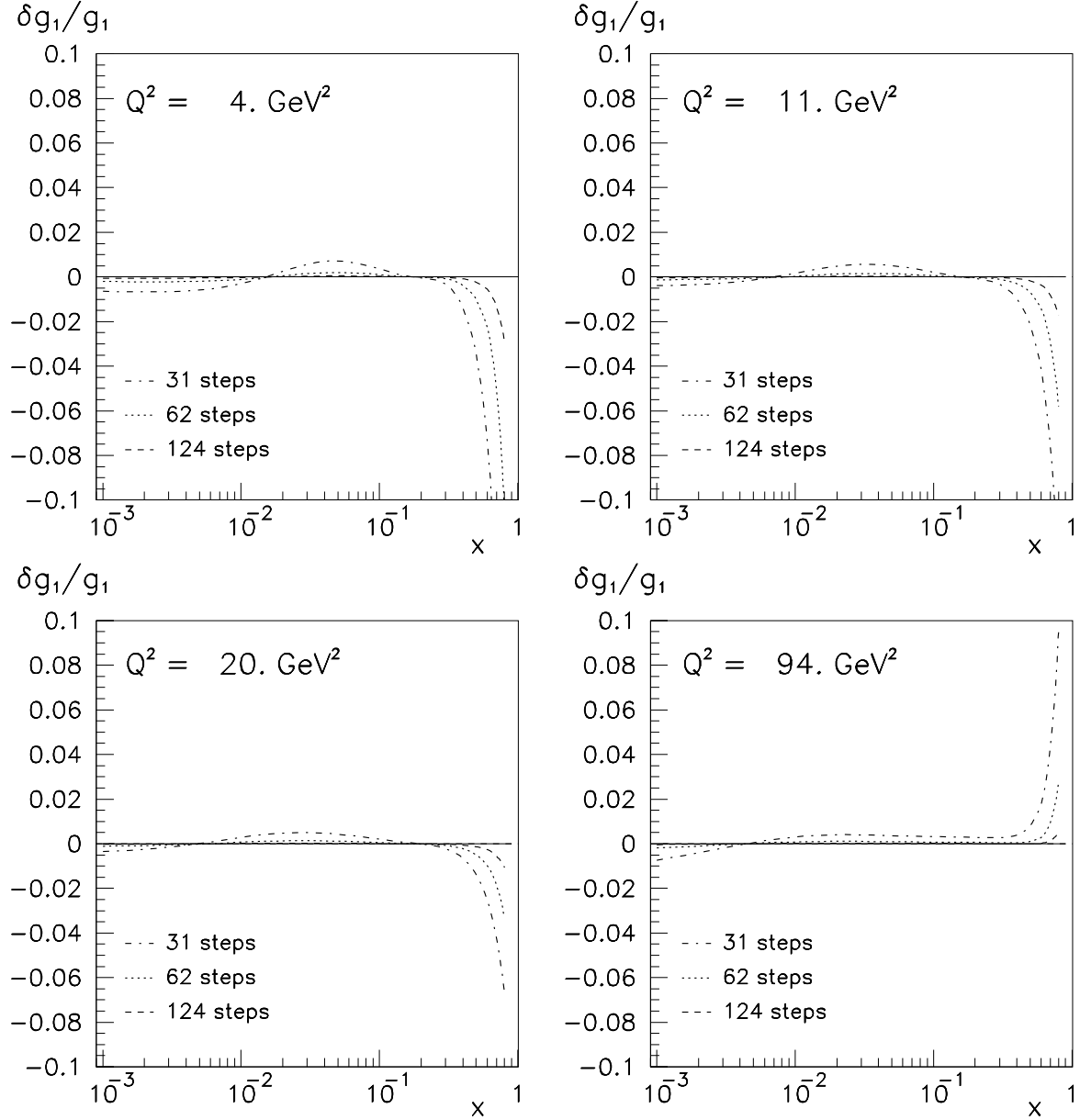


Figure 5: As in Fig. 1, but for the structure function  $g_1(x)$ . In this case the reference result was calculated with  $248 \ln(x)$  steps and  $50 \ln(Q^2)$  steps using the parton distributions of set A from [15] at  $4 \text{ GeV}^2$  as input.



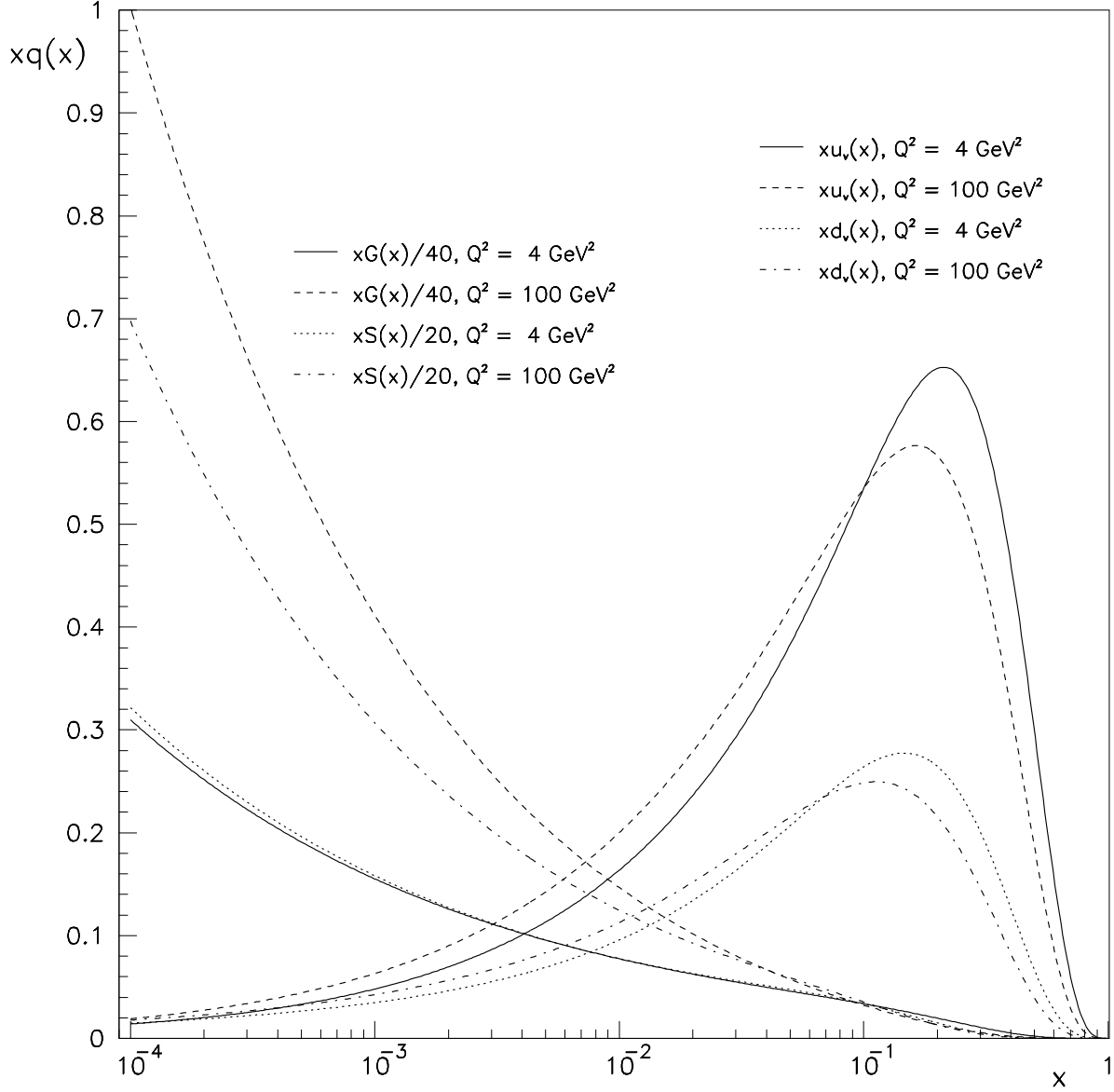


Figure 6: Parton distributions of the proton at the starting scale of  $4 \text{ GeV}^2$  and evolved to  $100 \text{ GeV}^2$ .

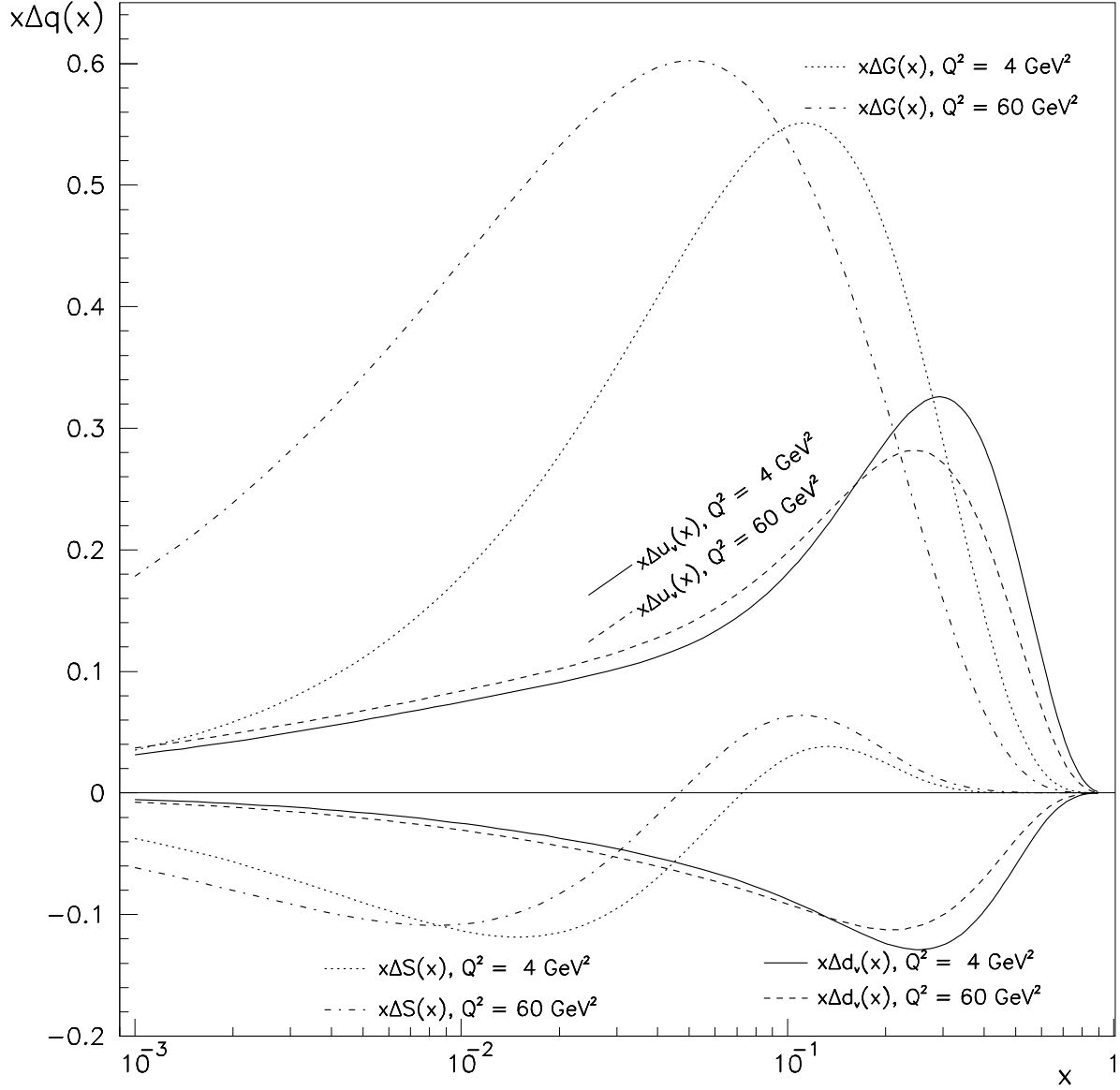


Figure 7: The polarization of the parton distributions of the proton at the starting scale of  $4 \text{ GeV}^2$  and evolved to  $60 \text{ GeV}^2$ .

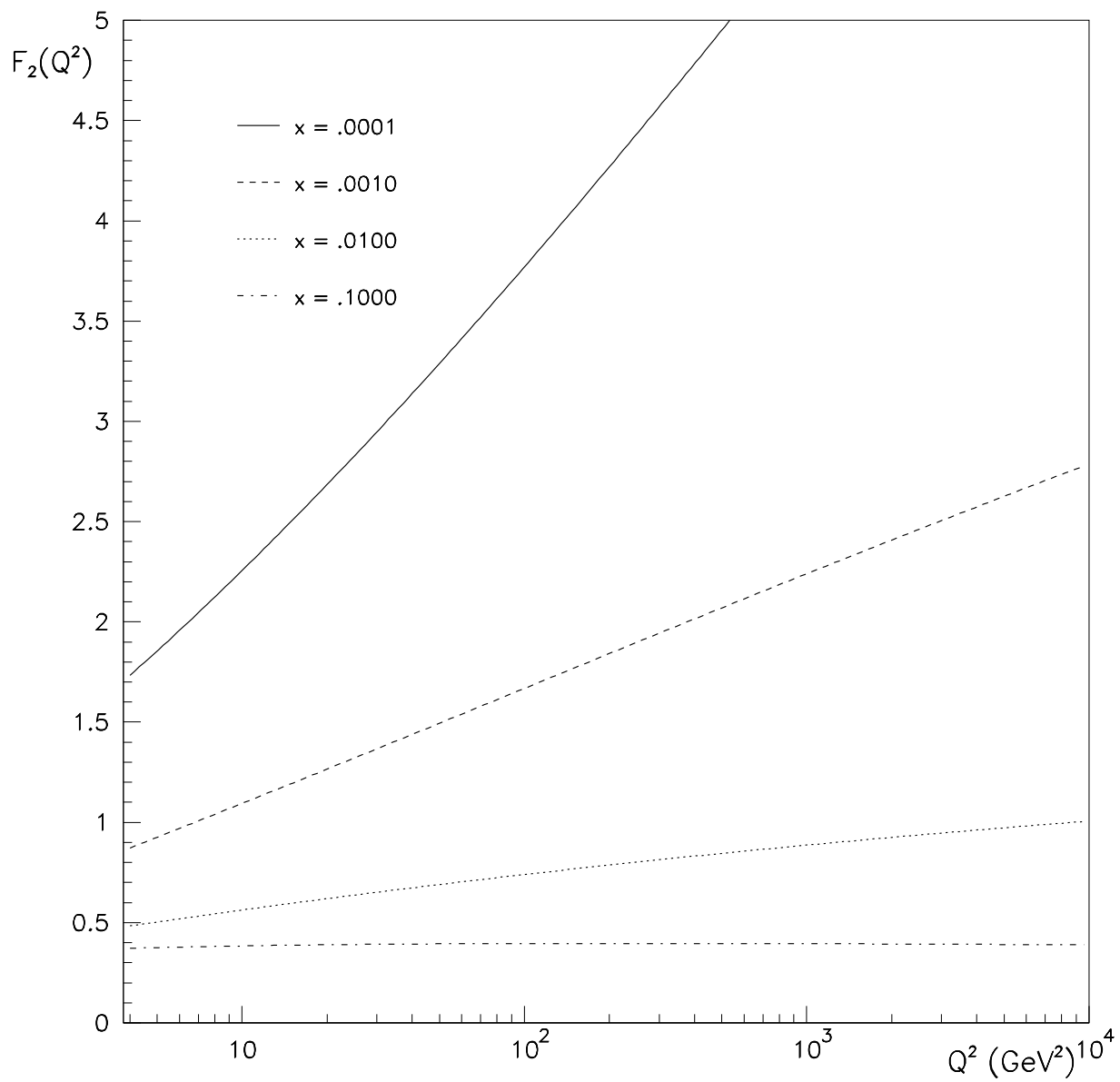


Figure 8:  $F_2(Q^2)$  at four  $x$  values.

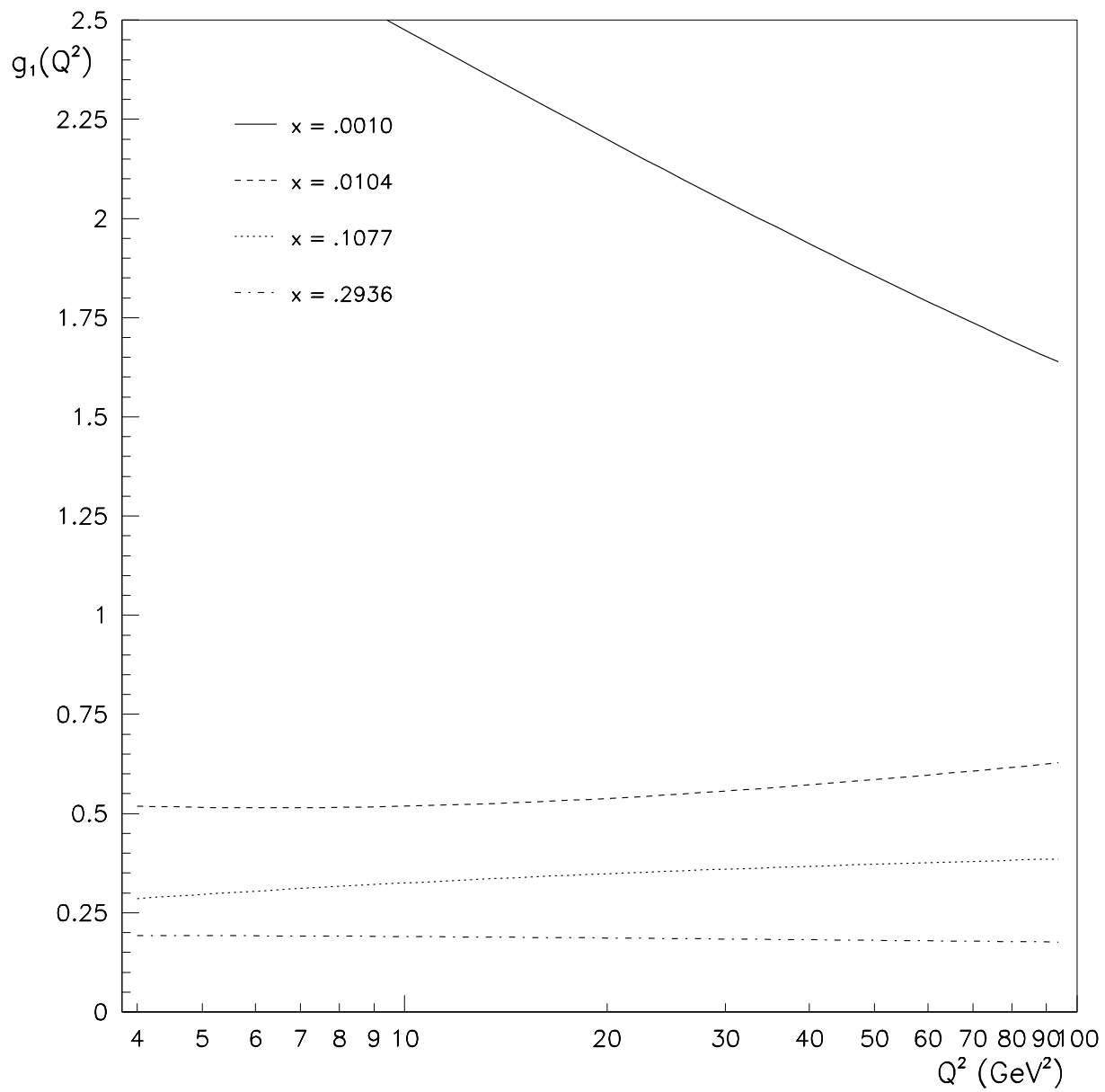


Figure 9:  $g_1(Q^2)$  at four  $x$  values.

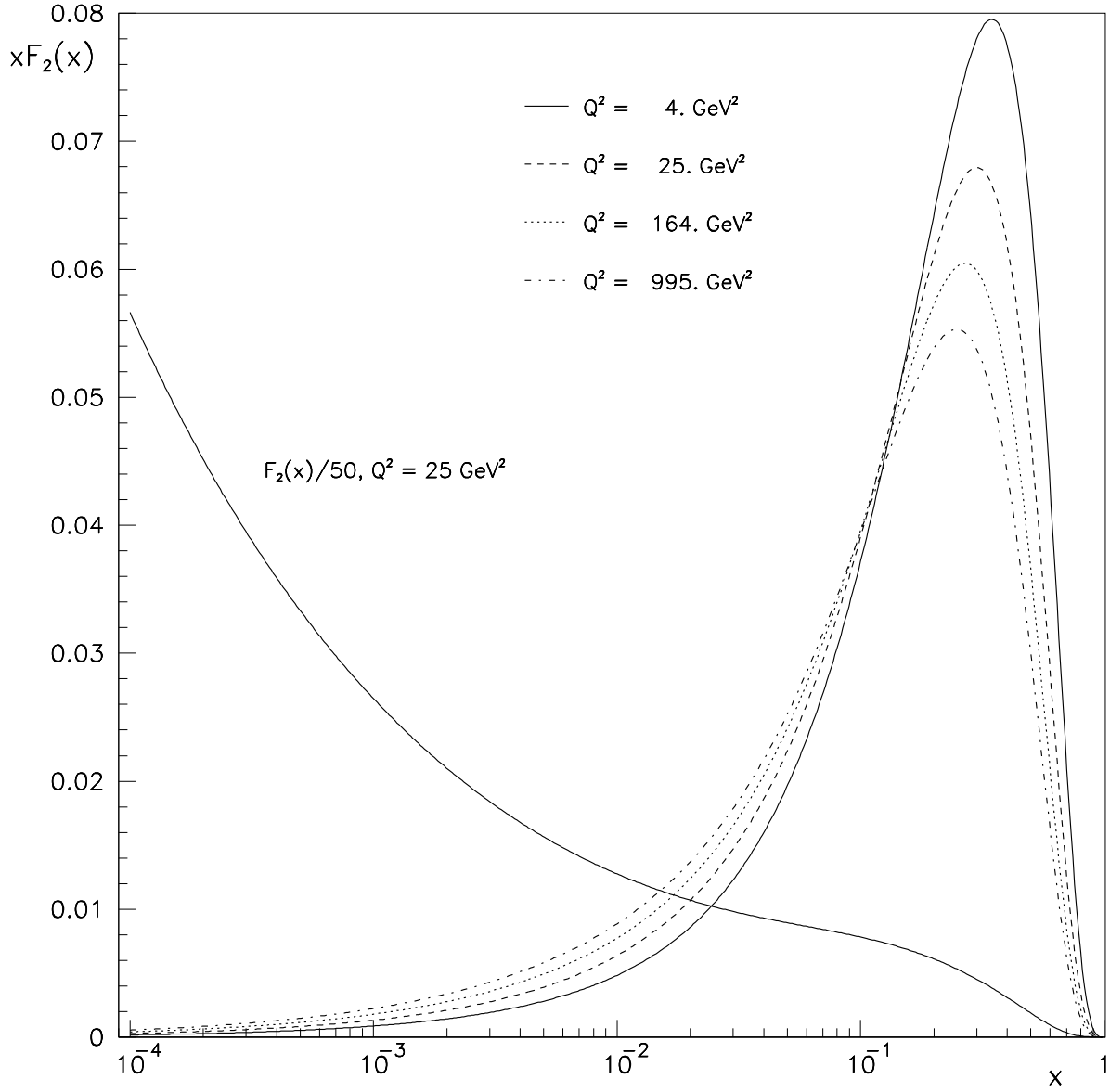


Figure 10:  $xF_2(x)$  at four  $Q^2$  values. Also plotted is  $F_2(x, 25 \text{ GeV}^2)$ .

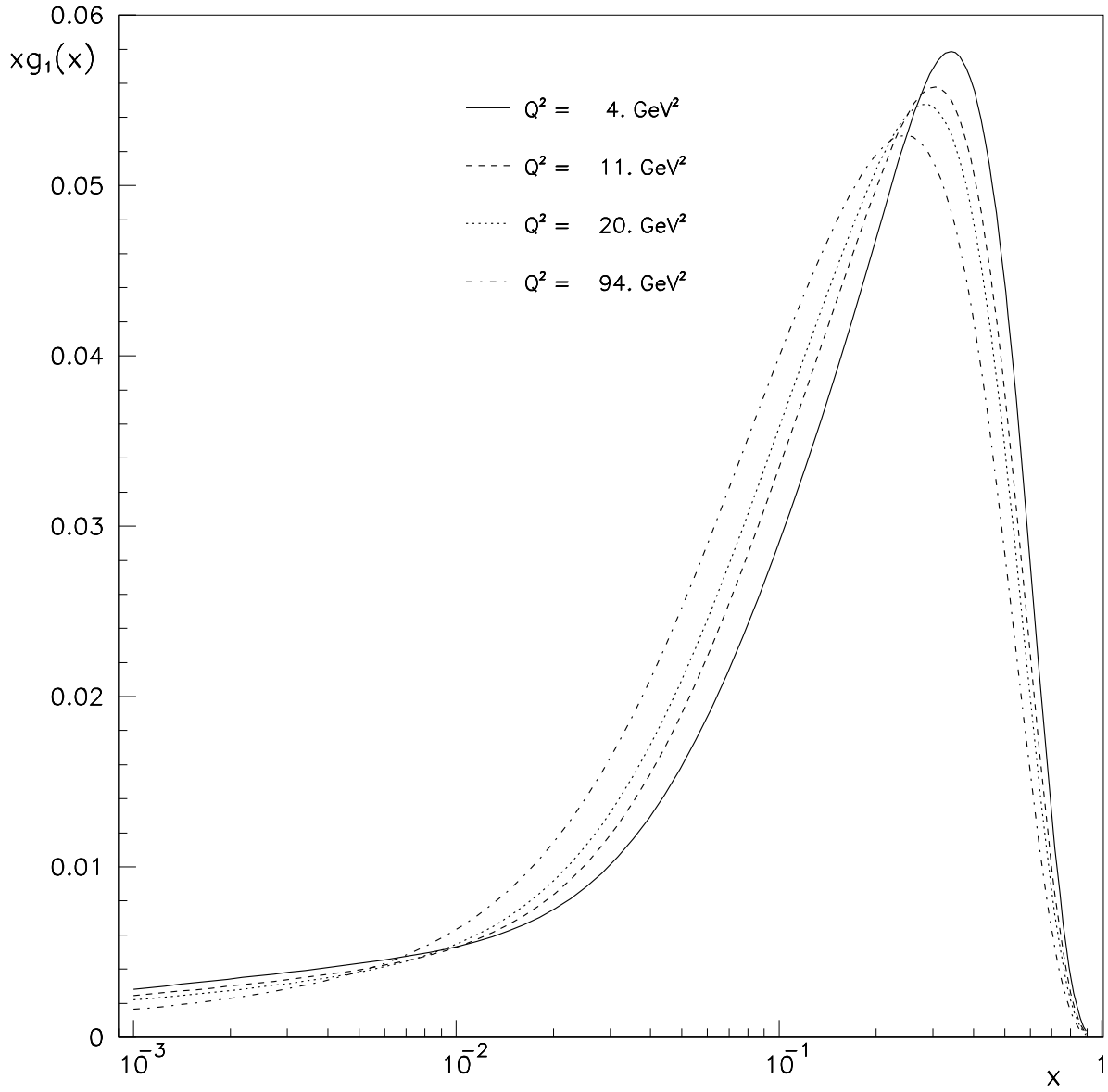


Figure 11:  $xg_1(x)$  at four  $Q^2$  values.